Microscopic Characterization of Nanocomposite based on the Mixture of Carbon Nanotube and Rosette Nanotube

J.-Y Cho[*], T. Yamazaki[*] , J.G. Duque[**], S. Doorn[**], S. Das[***], M. Green[***] and H. Fenniri[*]

[*]National Institute for Nanotechnology, National Research Council (NINT-NRC) and Department of Chemistry, University of Alberta, 11421 Saskatchewan Drive, Edmonton, Alberta T6G 2M9, Canada, jae-young.cho@nrc-cnrc.gc.ca, hicham.fenniri@nrc-cnrc.gc.ca

[**] Los Alamos National Laboratory, Physical Chemistry and Applied Spectroscopy (C-PCS) Group, Los Alamos, New Mexico 87544, USA

[***] Department of Chemical Engineering, Texas Tech University, 6th and Canton, Mail Stop 3121, Lubbock, TX 79409-3121, USA

ABSTRACT

In this paper, it was demonstrated that the self-assembled organic rosette nanotube (RNT) can encapsulate single-walled carbon nanotubes (SWNTs) and form nanocomposites. Importantly, the RNTs were found to hold their supramolecular architectures. To understand how nanocomposite forms, various cutting edge microscopic characterization methods were used, such as scanning electron microscopy (SEM), transmission electron microscopy (TEM), atomic force microscopy (AFM) and scanning tunneling microscopy (STM). Based on intensive microscopic analysis, two different models were suggested and modeled using molecular dynamic (MD) simulations.

Keywords: single-walled carbon nanotube, rosette nanotube, atomic force microscopy, scanning electron microscopy, transmission electron microscopy, scanning tunneling microscopy, molecular dynamics

1 INTRODUCTION

Single-walled carbon nanotubes (SWNTs) have attracted considerable attention in recent years due to their high electrical and thermal conductivity, chemical stability and exceptional mechanical properties. With these unique characteristics, SWNTs can be used in a wide range of applications in electronics, optics, and sensing. However, the inherent difficulties associated with the synthesis and separation of SWNTs pose serious obstacles to their further development. Notably, their dissolution and, purification, and separation in a suitable medium have been hampered. The ability to separate single SWNTs from the tight bundles they form would not only open new avenues in the field of nanotechnology, but is a necessary step for their proper chemical and physical examination and use [1-4].

Rosette nanotubes (RNTs) are assembled from a single bicyclic block with a guanine-cytosine (G∧C) base designed to have a hydrogen-bond donor-donor-acceptor array on one side and a complementary acceptor-acceptor-donor array on the opposite side. These building blocks assemble through H-bonds to form a six-membered rosette. The rosettes then π-π stack to form the nanotube, which has a hollow core and a length that can extend up to several micrometers [5-6].

In this study, we looked at the possibility of dispersing SWNT bundles using self-assembled RNTs. Our hypothesis was that the relatively apolar character of the RNT channel and its 1 nm cross section could accommodate SWNTs with the appropriate dimensions in water. Here we present convincing evidence (AFM, SEM, TEM and STM) showing the encapsulation of a SWNT inside an RNT as well as RNT growth on SWNT walls.

2 EXPERIMENTAL PROCEDURE

To make the nanocomposite, twin G∧C based RNT solution (1mg/ml in water) with two different batches of SWNTs, 187 and 164 which has a different average diameter, 0.9 nm and 0.76 nm repectively were prepared. After this, 1mg SWNT powder was added in solution and sonicated for 30 seconds. And then, centrifuged it and collected supernatant. For SEM and TEM study, two different TEM grids are used, thin-carbon-filmed 400 mesh grid and lacey carbon grid (Electron Microscopy Sciences). To prepare grids, a drop of solution was deposited and blotted using filtered paper after 10 s. SEM images were obtained from these grids without negative staining, at 10-30 kV accelerating voltage, 20 μA and a working distance of 5-8 mm on a high resolution Hitachi S-4800 cold field emission SEM. Energy filtered TEM (EF-TEM) and cryo-TEM investigations were also carried out on JEOL 2200 FS TEM - 200kV Schottky field emission instrument equipped with an in-column omega filter using Gatan CT 3500TR holder. Bright field TEM images are acquired using energy filtered zero loss beams (slit width 10ev) and low dose methods. For AFM and STM study, both clean mica and HOPG (highly ordered pyrolytic graphite) substrates (1×1 cm^2) were prepared and the samples were deposited by spin-coating at 3500 rpm for 30 s to remove the excessive precipitation from the surface of sample. Sample surface was observed using a Digital Instruments/Veeco Instruments MultiMode Nanoscope IV AFM equipped with an E scanner. For getting optimized height profile in this investigation, silicon cantilevers (MikroMasch USA, Inc.) with low spring constants of 4.5 N/m were used in tapping

mode (TM-AFM). To obtain a clear image from surface, low scan rate (0.5-1 Hz) and amplitude setpoint (1V) were choose during measurement. To have a detail molecular structure of sample, ambient STM was performed using MultiMode Nanoscope IV AFM equipped with an A scanner. In this investigation, mechanically fabricated PtIr tips from wire (Nanoscience, Pt_8Ir_2, 0.25mm diameter) were used with slow scan rate (1.98Hz). Bias was 1V and current setpoint was 300 pA. Both integral gain and proportional gain were 0.5 for constant current mode.

3 RESULTS AND DISCUSIONS

To understand the morphological changes of RNTs and SWNTs after mixing, four different samples, RNTs only, SWNTs only and SWNT-RNT nanocomposites in the different batches (187 and 164) are prepared on carbon filmed TEM grid and imaged by SEM, as shown in Figure 1. Generally, RNT samples show very long and flexible wire-like structures (Figure 1a) and SWNT samples show long and tightly bundled ropes of SWNTs (Figure 1b). However, after mixing RNTs and SWNTs, the SWNT bundles dissociated and appeared as bright lines as shown in Figure 1c and d (due to enhanced electron scattering). On the other hand, RNTs show mixture morphology, many short broken tubes along with long tubes after mixing. Interestingly, we can see the relatively long tubes in the batch 187 (Figure 1c), but very short tubes which stick to the surface of SWNTs perpendicularly in the batch 164 (Figure 1d). This may indicates that the most of G-C bases are used for detaching and encapsulating SWNTs, and the rest of them remain as short tubes which attached the thicker SWNTs perpendicular.

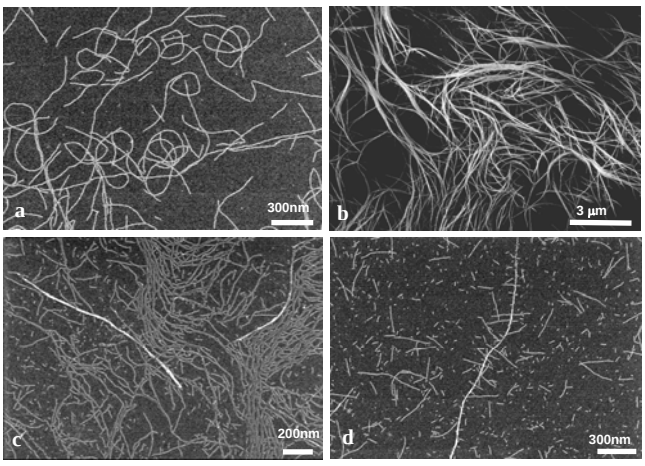

Figure 1. SEM observation of the morphological changes after mixing RNTs and SWNTs: a) RNTs, b) SWNTs, c) SWNT-RNT nanocomposites in the batch 187 and d) 164 (bright white line is the bundle of SWNTs and dark gray line is RNTs).

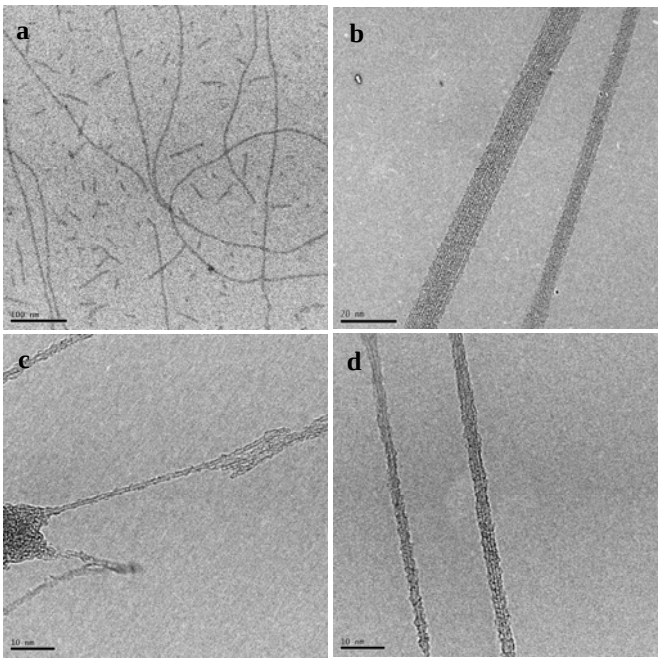

Figure 2. TEM Images from a) RNTs, b) SWNTs, c) SWNT-RNT nanocomposites in the batch c) 187 and d) 164.

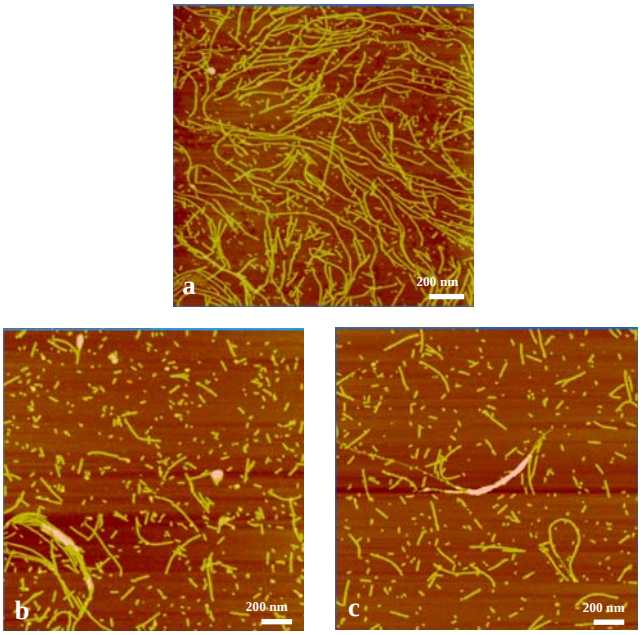

Figure 3. AFM images from a) RNTs b) SWNT-RNT nanocomposites in the batch 187 and c) 164 (bright line is the bundle of SWNTs).

To understand the detail relationship between SWNTs and RNTs, cryo-TEM was used since it has minimum beam damage to the soft organic nanostructures. As shown in Figure 2, RNTs show long individual tubes (Figure 2a) and SWNTs are tightly bundled (Figure 2b). After mixing, they are detached from the bundle (Figure 2c and d), and the

outside of SWNTs are coated by G-C bases regardless of bundle. Especially, as shown in Figure 2d, the bigger SWNT (164) show more the bundle of SWNT than the smaller one (187). This finding support that it is not easy process for the bigger one to be totally encapsulated by G-C bases and form the rosette outside of SWNT. The measured diameter for the SWNT was 0.79 ± 0.09 nm and for the RNTs it was 3.44 ± 0.42 nm.

The SWNT-RNT nanocomposite was also characterized by TM-AFM. As shown in Figure 3, the same morphological changes were observed with SEM and TEM. The measured height value (corresponding to the diameter) of the RNTs was 3.09 ± 0.44 nm, which is lower than the calculated and the measured TEM values as a result of a compression under the AFM tip. However, the SWNT-RNT nanocomposites had a height of 3.46 ± 0.24 nm, similar to the diameter measured by TEM. This result suggests that the encapsulation of the SWNTs by the RNTs can minimizes the compressibility because of increasing rigidity by filling the inner channel of RNT.

To verify this finding, STM was performed on the nanocomposite sample on HOPG surface, as shown in Figure 4. It was clearly seen the dark line in the middle of tubes which is SWNT exist. The measured diameter is around 0.789 nm which is well matched with the value from TEM. The diameter of nanocomposite is around 3.747nm which is also well matched with measure diameter by AFM. Also, the helical structure from the surface of nanocomposite was clearly observed, as indicated by arrows. It might be critical evidence that RNT accommodates the SWNT by encapsulating and sustains its supramolecular structure we designed.

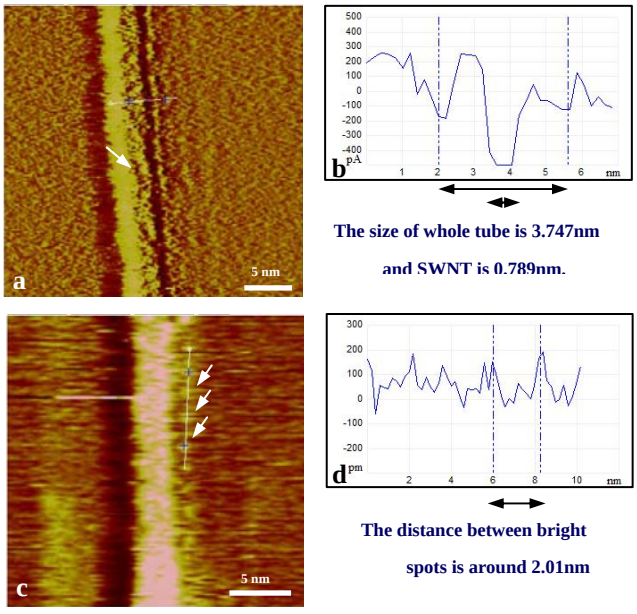

Figure 4. STM results of SWNT-RNT nanocomposite on HOPG: a) current profile b) cross -sectional profile of drawn line in Figure 4a c) height profile and d) cross -sectional profile of drawn line in Figure 4c.

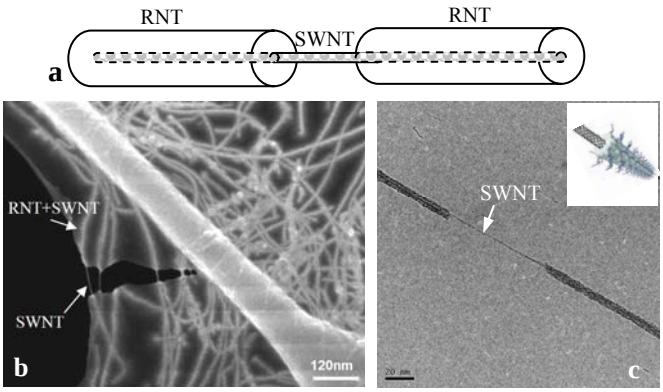

Figure 5. The encapsulation of the SWNTs by the RNTs (Model 1): a) schematic diagram, b) SEM and c) cryo-TEM image.

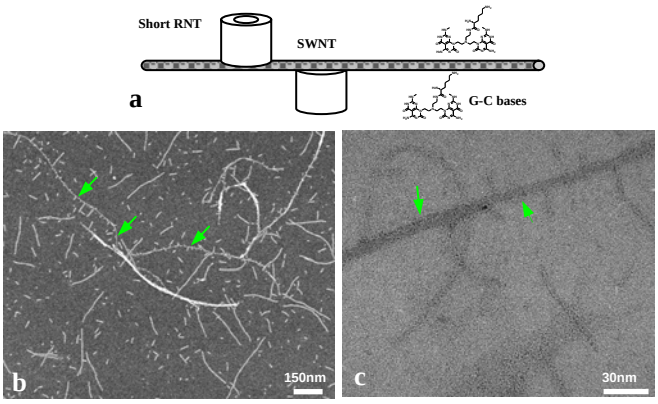

Figure 6. RNTs growing perpendicularly to the main axis of the SWNTs (Model 2): a) schematic diagram, b) SEM and c) EF-TEM image.

Based on these findings from the different microscopic techniques, two possible models which can explains the formation of nanocomposite are suggested as follow. At first, SWNT can be located inside of channel of RNT (model 1), as shown in Figure 5a. As an evidence of this, SEM image (Figure 5b) shows smaller SWNTs make a good mixture with RNT. However, when it is ruptured, relatively weak RNT is broken, but strong SWNT can survive, as shown in Figure 5b and c.

Another way of explanation on the nanocomposite formation can be that the top of RNT vertically stick to the surface of SWNT, whether is short RNT or G-C bases (Figure 6a). These findings are observed by SEM and TEM, as shown in Figure 6b and c. It was clearly seen the SWNT has tiny bumps which is the vertical growth of G-C bases or short stack of rosettes, as indicated by arrows (model 2). It was observed that model 2 is more dominant in a bundle than individual SWNT.

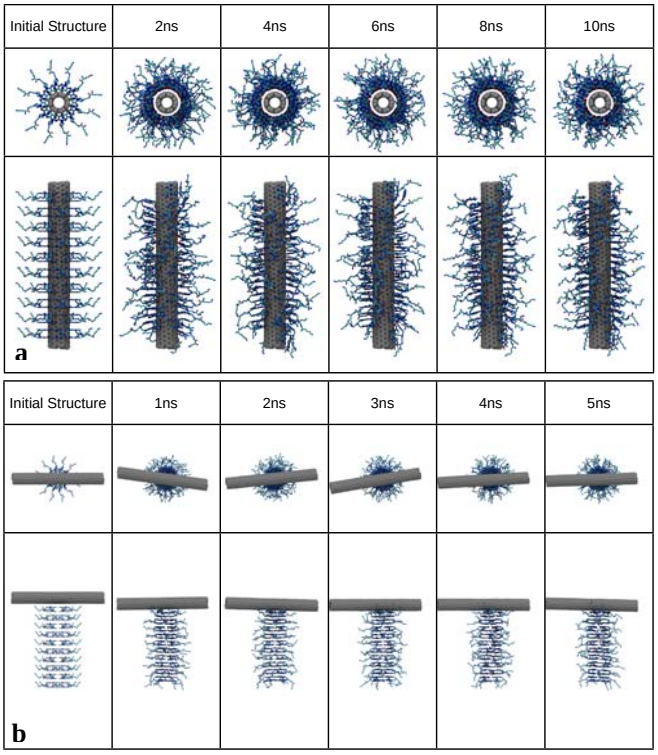

Figure 7. MD simulations for the nanocomposite between RNT and SWNT, a) models 1 and b) 2

To support these models drwan from microscopic characterization, molecular dynamics (MD) simulations was performed, as shwon in Figure 7. Our MD simulation supports that the RNT-SWNT nanocomposite is built based on the wrapping mechanism in which isolated G-C bases separately attach onto the SWNT surface and finally form the tubular supramolecular architecture around SWNT, rather than the penetration of SWNT inside the RNT channel. Furthermore, the simulation trajectories indicate that the π-π interaction between G-C base and SWNT surface competes with the interactions among G-C bases. When one G-C base attaches to the SWNT surface, it readily falls down onto the SWNT surface to have the π-π interaction. However, when the G-C base forms the hydrogen bond and/or π-π interaction with other bases, we observed that G-C bases do not immediately fall down onto the SWNT surface, suggesting the cluster of the G-C bases forming these intermolecular interactions may behave as the nucleation point for the RNT's tubular supramolecular architecture.

4 CONCLUSION

Based on extensive microscopic characterization and modeling, it can be concluded the self-assembled RNT wraps SWNT to form the RNT-SWNT nanocomposite and disperses SWNTs. Two different models are suggested to explain the formation of nanocomposite: SWNT is located inside of the RNT channel in the model 1, while RNT stick to the top of SWNT in the model 2. Combining both models 1 and 2, it can be explained that RNT plays a key role in detaching the SWNT from the tight bundle and produces nanocomposite by coating with G-C bases (whether it is single or multiple SWNTs) for the further applications.

ACKNOWLEDGEMENTS

We thank the National Institute for Nanotechnology and the National Research Council CANADA for supporting this program.

REFERENCES

[1] Juan G. Duque, A. Nicholas G. Parra-Vasquez, Natnael Behabtu, Micah J. Green, Amanda L. Higginbotham, B. Katherine Price, Ashley D. Leonard, Howard K. Schmidt, Brahim Lounis, James M. Tour, Stephen K. Doorn, Laurent Cognet, and Matteo Pasquali, Diameter-Dependent Solubility of Single-Walled Carbon Nanotubes, ACS Nano, 4 (6), 3063–3072, 2010

[2] Adreas Hirsch, Angew. Chem. Int. Ed. 41, 1853–1859, 2002

[3] Howard Wang, Curr. Opin. Colloid Interface Sci. 14, 364–371, 2009

[4] Claudia Backes, Cordula D. Schmidt, Karin Rosenlehner, Frank Hauke, Jonathan N. Coleman, and Andreas Hirsch, Adv. Mater. 22, 788–802, 2010

[5] Jesus G. Moralez, Jose Raez, Takeshi Yamazaki, R. Kishan Motkuri, Andriy Kovalenko, and Hicham Fenniri, J. Am. Chem. Soc. 127, 8307-8309, 2005

[6] Jae-Young Cho and Hicham Fenniri, Imaging & Microscopy, 12 (4), 33-35, 2010